

LARGE FORMAT LI CO-DOPED NaI:Tl (NaIL™) SCINTILLATION DETECTOR FOR GAMMA-RAY AND NEUTRON DUAL DETECTION

P.R. Menge, K. Yang, and V. Ouspenski
Saint-Gobain Crystals
Hiram, OH, USA

ABSTRACT

Li co-doped NaI:Tl (NaIL™) is a potentially game-changing scintillation material for gamma-ray and neutron dual detection. Li co-doping introduces efficient thermal neutron detection to one of the most well-established gamma-ray scintillators while retaining the favorable scintillation properties of standard NaI:Tl. NaIL exhibits excellent neutron-gamma pulse shape discrimination (PSD) capability with PSD figure of merit between 2 and 4. Simulations show that NaIL detectors with only 1 - 3% of enriched ⁶Li doping can outperform many existing neutron detection solutions such as standard ³He tubes or CLYC scintillator in terms of neutron detection capability. NaIL will be the first spectral gamma-neutron dual mode detector available in large formats, i.e. multi-liter crystal sizes. Saint-Gobain Crystals is actively working on industrialization of this material. Large format NaIL prototype detectors have been fabricated and tested.

INTRODUCTION

Much current interest exists for radiation detection materials capable of simultaneously identifying gamma rays and neutrons. Neutron sensitive scintillators have been heavily studied recently due to the ³He crisis and the increasing demand from security applications¹. In particular, Li-containing elpasolites such as Cs₂LiYCl₆ (CLYC) and Cs₂LiLaBr₆ (CLLB) have garnered interest because of their capability of neutron and gamma dual detection with pulse shape discrimination (PSD)²⁻⁶. However, due to cost and complexity in quaternary crystal growth, commercially available elpasolite scintillators such as CLYC are limited to approximately $\varnothing 3 \times 3$ "⁷ and thus, are not available in the large sizes necessary for portal monitors at border crossings, for bulk cargo scanning or for vehicle-mounted area monitors. NaI(Tl), however, is routinely grown by Saint-Gobain in ingots exceeding 100 liters in volume. NaI(Tl) can be engineered to be neutron-sensitive by incorporating Li into the crystal matrix. Previously, we have reported on crystal sizes up to $\varnothing 2 \times 2$ " (0.1 liter) with ⁶Li co-doping (commercially named NaIL™)⁸. NaIL exhibits excellent neutron-gamma PSD with a high figure-of-merit⁹. Measurements show that large NaIL detectors need only 1 - 3% of ⁶Li doping to outperform many existing neutron detection solutions such as standard ³He tubes or CLYC scintillator in terms of performance and cost¹⁰. This report documents the progress made on large crystals, their absolute neutron detection efficiencies and the first measurements of a large NaIL crystal (2000 cm³).

According to the NaI-LiI phase diagram, NaI can form a solid solution with up to 100% LiI¹¹. Thus, it is possible to introduce a significant amount of Li into the matrix of NaI without interrupting its crystalline structure. Previously, we have reported grown single crystals of NaI(Tl) co-doped with Li at concentrations up to 8 mol% (with respect to Na)⁸. However, concentrations of ⁶Li do not need to be this high if the crystal is large. The neutron detection efficiency is dependent on the areal density of ⁶Li. Source detection capability is dependent on the solid angle presented by the detector multiplied by neutron detection efficiency. Therefore, NaIL crystals with large thicknesses and large cross-sectional areas can lead to extremely capable dual gamma/neutron detectors. A simple calculation using thermal neutron absorption cross-sections illustrates this concept. Figure 1 plots thermal neutron detection capability

(efficiency * area) vs NaIL crystal thickness and lithium concentration. It assumes a NaIL crystal with cross-section of 10x40 cm², which is a common industrial size. As the thickness of the crystal increases, so does the thermal neutron detection. At a thickness of 5 cm and [⁶Li] = 1%, the NaIL crystal reaches about 1/3 that of a large ³He tube (ø5x173 cm, 3 atm), a typical neutron detector used for vehicle scanning at U.S. border crossings.

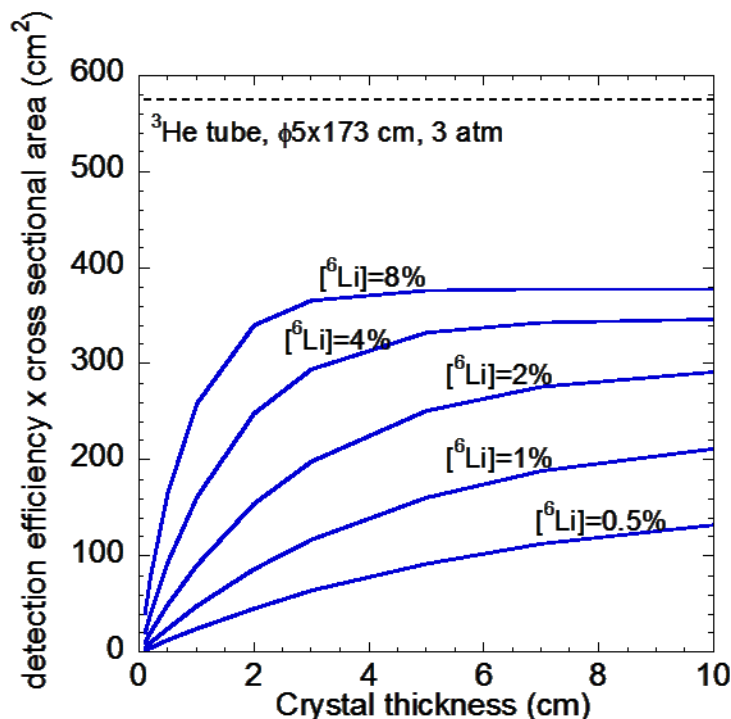


Figure 1. Thermal neutron detection capability vs. NaIL crystal thickness and lithium concentration for a 400 cm² crystal surface. The values are calculated from thermal neutron interaction cross-sections.

EXPERIMENTAL

Experimental Methods

NaIL single crystals studied in this research were grown by Saint-Gobain Crystals. Thallium concentration was fixed at 0.1 at% in the melt for all grown crystals. Li concentration was varied between 0 – 8 at. % in order to study its effect on the scintillation performance and neutron detection efficiency. All Li concentrations in the crystal presented here are at. % with respect to Na. The values are verified by inductively coupled plasma – optical emission spectrometry (ICP-OES). NaI raw material is originated from the production purification process of Saint-Gobain Crystals. LiI salts enriched to 95% ⁶Li are purchased from SAFC Hitech with at least 99.99% purity. All NaIL crystals appear clear and colorless. No cloudiness, precipitation or phase separation was observed even for the highest doping level.

Scintillation light was detected with a Photonis XP20Y0 photomultiplier tube. Scintillation pulses were collected and analyzed for light yield and energy resolution with a multichannel analyzer (Aptek model S5008, bi-polar shaping, 1 μs shaping time, 11-bit digitization). Scintillation pulses were digitized for PSD analysis using a waveform digitizer (CAEN model DT5720, 250 MS/s, 12 bit digitization).

Neutron Detection Capability

Adding Li to the NaI(Tl) matrix increases the length of the scintillation pulse. The more that is added, the longer the pulse becomes. The lengthening of the pulse is believed to be caused by the additional electron traps created by the lithium atoms distorting the crystal lattice. The traps are shallow enough to eventually release their electrons, but this delay causes an increase in the pulse length. Interestingly, pulses created by interactions with gamma rays create more of an increase than do interactions with neutrons. This difference can be used to separate gamma ray detection events from neutrons. Figure 2 shows representative scintillation pulses from gamma rays and neutrons for three different Li concentrations.

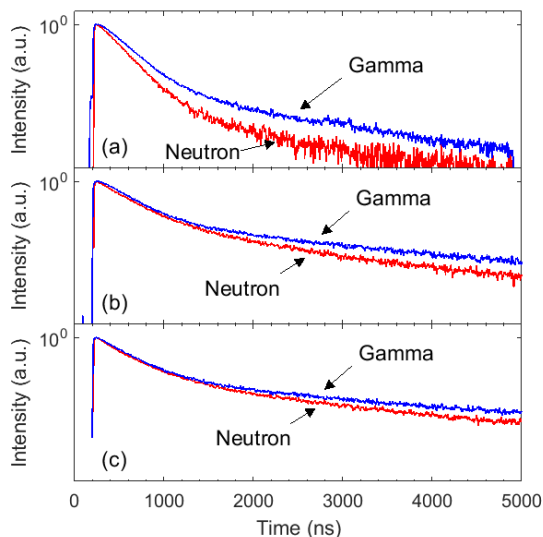


Figure 2. Averaged gamma-ray and neutron scintillation pulses for NaIL crystals with (a) 0.7% Li, (b) 2.2% Li and (c) 7.7% Li.

Note in Figure 2 that as [Li] increases the difference in pulse shape between neutrons and gamma rays decreases. Nevertheless, even at [Li]=7.7%, enough difference exists to easily discriminate neutrons from gammas. Figure 3 illustrates the separation clearly. This figure shows data taken on a $\varnothing 2.5 \times 2.5$ cm crystal with [Li]= 0.6%. The radiation source was ^{252}Cf which emits gamma rays and spontaneous fission neutrons. The neutrons were moderated with 5 cm of polyethylene. The x-axis represents the gamma equivalent energy of each individual pulse. Specifically the x-axis is $\text{Energy} = \int_0^{1600\text{ns}} S(t)dt$, where $S(t)$ is the photosensor signal at time t . Note the signal from $^6\text{Li}(n,t)\alpha$ reaction appears at about 3.4 MeV gamma equivalent energy. The y-axis is the PSD value of the scintillation pulses. The PSD value is the ratio of the amount of light contained at the end of the pulse divided by the total amount of light emitted. This is a traditional PSD technique termed “tail-to-total”¹². Specifically in Figure 3, the PSD value is calculated for each pulse using:

$$PSD = \frac{\int_{400\text{ns}}^{1600\text{ns}} S(t)dt}{\int_0^{1600\text{ns}} S(t)dt} \quad (1)$$

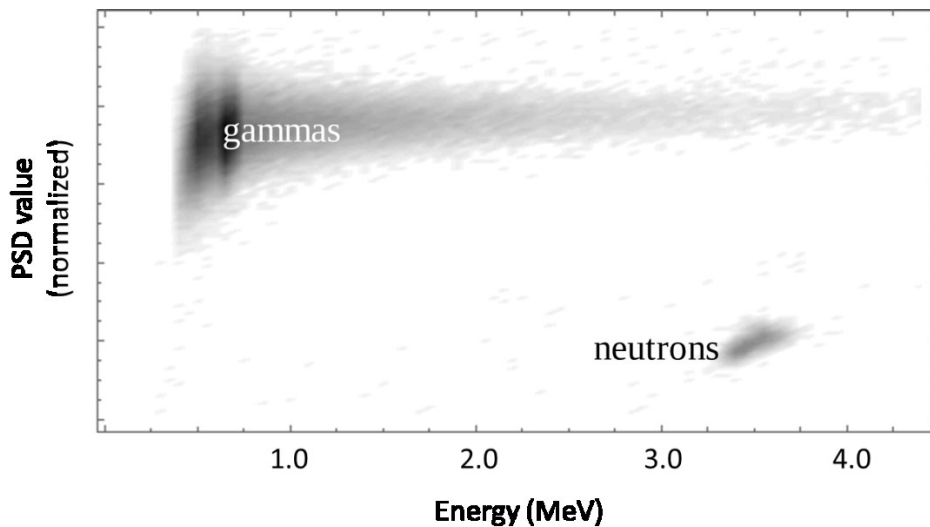


Figure 3. PSD-energy density contour plot for NaIL scintillation waveforms under irradiation from a moderated ^{252}Cf source. Note the good separation between neutrons and gammas.

The quality of PSD is often described using a figure-of-merit (FoM) which quantifies the degree of signal separation⁹. The data in Figure 3 exhibit an FoM=4.3. A rule-of-thumb is that when the PSD FoM is greater than 1.5, then for most practical purposes, complete separation of gammas and neutrons can be obtained⁴.

Neutron Detection Efficiency

Two NaIL crystals of different size and lithium content were measured for neutron detection efficiency at The Ohio State University Nuclear Reactor Laboratory (OSU-NRL). The crystals were measured using beams of thermal neutrons with known fluxes. Table I shows the crystal sizes, the lithium concentration, the measured thermal neutron detection efficiency, and the predicted efficiency from MCNPX simulations¹³. The slight discrepancies between measured and calculated efficiencies are presumed due to small [^6Li] differences between the samples that underwent ICP-OES and the actual crystals. The samples were taken from the ingots in positions adjacent to those from which the detector crystals listed below were cut. The detector crystals themselves have not undergone ICP-OES, since this is a destructive test. Figure 4 shows a plot of detected neutron count rate vs. the neutron particle flux intercepted by the crystals. The slopes of the fitted lines indicate the detection efficiency.

Table I. NaIL calibrated thermal neutron measurements

Crystal name	Size	^6Li concentration in crystal	Thermal neutron detection efficiency	MCNPX efficiency prediction
F24-35A	ø2.5x2.5 cm	1.37%	34.5±0.2%	32.8%
F12-01C	ø5.1x5.1 cm	0.23%	10.6±0.3%	11.1%

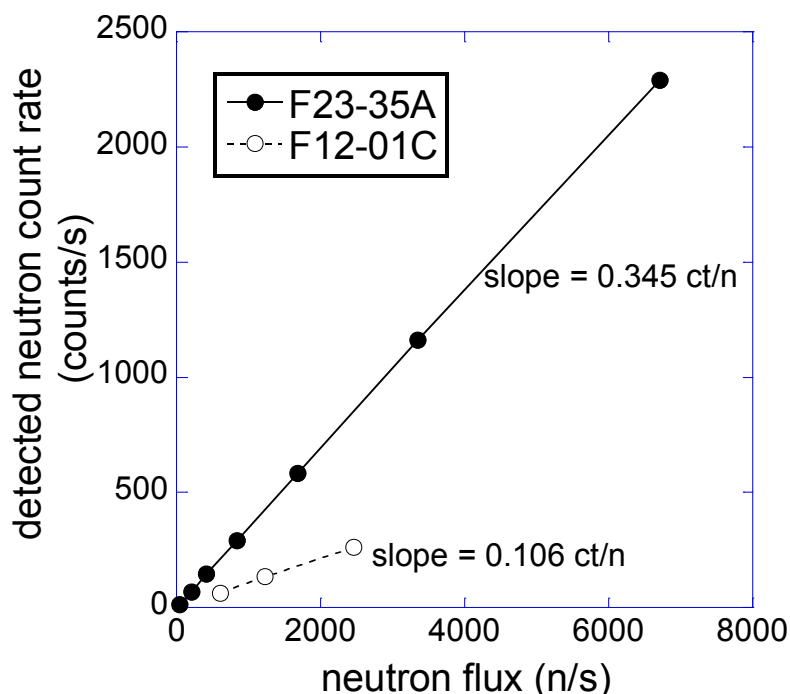


Figure 4. Plot of the detected neutron count rate vs the thermal neutron flux from the OSU-NRL reactor beam. The NaIL crystal, F23-35A, has dimensions $\varnothing 2.5 \times 2.5$ cm and $[^6\text{Li}] = 1.37\%$ (filled circles). F12-01C has dimensions $\varnothing 5.1 \times 5.1$ cm and $[^6\text{Li}] = 0.23\%$ (open circles).

The important points to note regarding Table I and Figure 4 are that even at the low concentration of $[^6\text{Li}] = 1.37\%$, neutron detection efficiency is a significant 34.5%, which corresponds well to prediction. Although F12-01C has only $\sim 1/6$ the ^6Li concentration of F23-35A, it has $1/3$ the efficiency because of its greater thickness. These points are illustrative of a unique advantage of NaIL. The neutron absorption cross sections of the other two main constituent elements, Na (0.53 barn) and I (6.15 barn), are significantly smaller than that of ^6Li (940 barn)¹⁴. This enables the use of low Li concentrations and large thicknesses to achieve the same neutron detection capabilities as ^3He or CLYC or CLLB detectors.

Scintillation Light Yield and Energy Resolution

Scintillation light yield and energy resolution of NaIL with different Li concentrations are shown in Figure 5. Compared with standard NaI:Tl, both light yield and energy resolution of NaIL gradually degrade with increasing Li concentration. NaIL crystals show a light output $\sim 34,000$ photons/MeV with 1% Li doping and $\sim 31,000$ photons/MeV with 2% Li doping. The scintillation light yield is still above 30,000 photons/MeV for the NaIL crystal containing 7.7% Li. On the other hand, energy resolution of NaIL does not appear strongly dependent on the Li doping concentration, at least for crystals with Li concentration under 8%. The averaged energy resolution of NaIL is stabilized around 7% for in a wide range of Li concentrations.

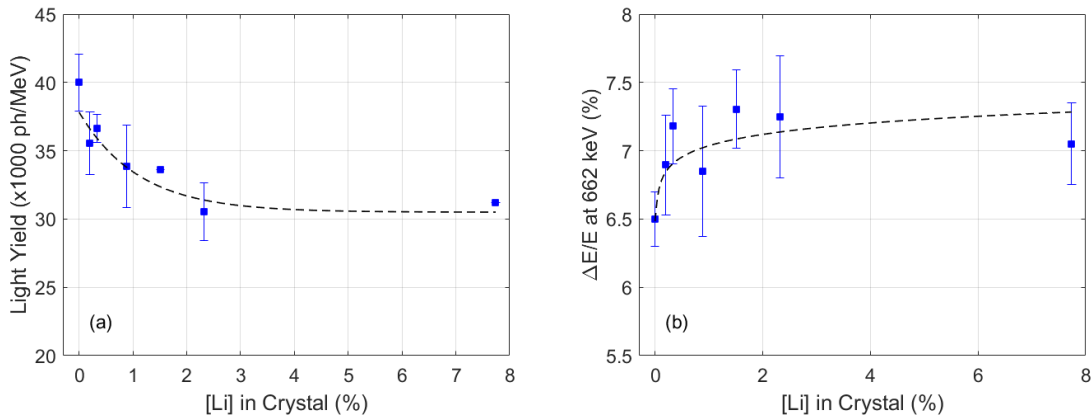


Figure 5. (a) Scintillation light yield and (b) energy resolution (at 662 keV) of NaIL with different Li concentrations in crystal

Degradation in the scintillation performance of NaIL can be attributed partially to decreased intrinsic scintillation efficiency and partially to the variability in the crystal synthesis process. The results presented in Fig. 5 are averages of 20 crystals. In terms of best results, we were able to achieve an energy resolution of 6.3% with 1% Li doping and 6.6% with 2% Li doping. It is expected that light yield and energy resolution of NaIL will be improved with further crystal growth process refinements.

Figure 5 indicates a potential problem of growing crystals with low lithium concentration. The greatest dependence in light yield and energy resolution occur at these low values. Therefore, even small lithium concentration gradients can cause significant non-uniformities within an ingot or a large crystal. These non-uniformities can degrade energy resolution and possibly the quality of PSD since it also changes with [Li] (see Figure 2).

Performance of a Very Large NaIL Crystal

A very large NaIL ingot, $\varnothing 80 \times 23$ cm, with $[^6\text{Li}] = 1\%$ in the melt (added as ^6LiI) was recently grown. A standard production furnace has been specifically dedicated to NaIL growth so that general NaI(Tl) production is not contaminated with Li. The crucible is covered with a lid to suppress evaporation of the the LiI. The grown ingot was cut into several large crystals. Figure 6a is a photo of a $5.1 \times 10.2 \times 40.6$ cm³ crystal cut from the ingot and then sealed in a housing as shown in Fig. 6b.

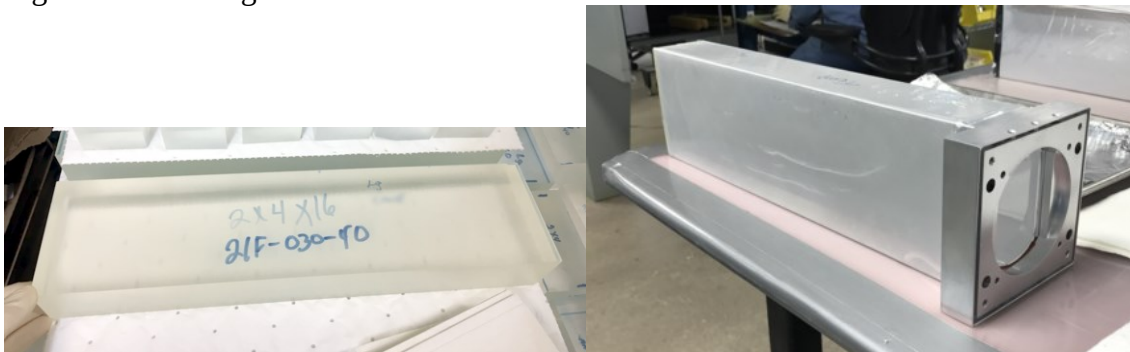


Figure 6. a) photo of a large (~ 2100 cm³) crystal cut from a $120,000$ cm³ NaIL ingot. b) the same crystal packaged in a hermetic housing for testing.

The gamma ray energy resolution measured with a side-on 662 keV source was 9.8%. A typical energy resolution for a standard NaI(Tl) crystal of this size and manufacture is 7.0 - 8.0%. The cause of the worsening is due to non-uniformity in light yield which is mostly due to

a non-uniformity in [Li] from one end of the crystal to the other. ICP-OES tests on samples adjacent to each crystal end measured $[\text{}^6\text{Li}] = 0.25\%$ and $[\text{}^6\text{Li}] = 0.47\%$. Thus, based on Figure 5, a light yield non-uniformity of about 5% can be expected. This additional broadening is believed to be the cause of most of the worsening.

Neutron data were collected using a ^{252}Cf source moderated by 5 cm of polyethylene and placed 2 m from the detector. The PSD-energy plot is shown in Figure 7.

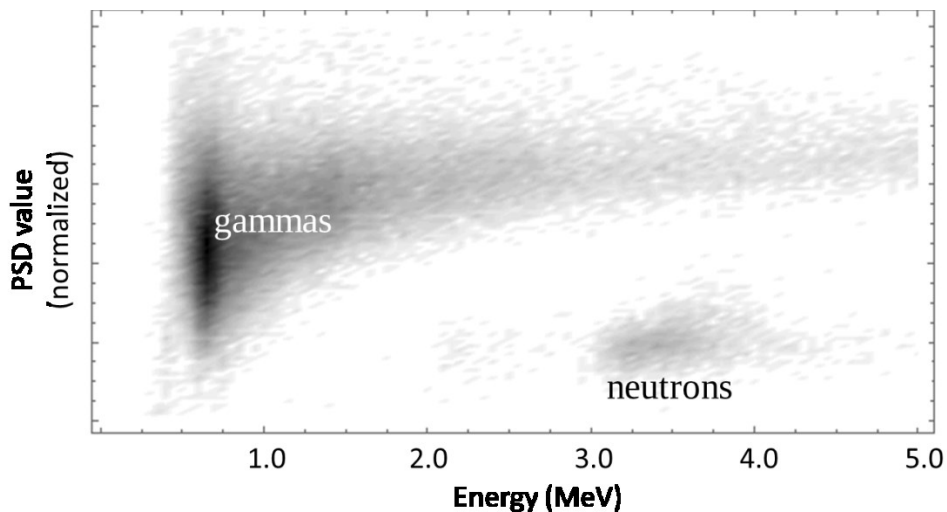


Figure 7. PSD and energy density contour plot for a large NaIL crystal ($\sim 5 \times 10 \times 40 \text{ cm}^3$) irradiated with a moderated ^{252}Cf source.

Although the quality of PSD is not as good as the small crystal shown in Figure 3, it is still an impressive $\text{FoM} = 2.0$. This is good enough to ensure that a gamma ray is mistaken for a neutron at a rate of less than 10^{-7} per gamma detection. The neutron detection rate was 0.40 count/s/ng of ^{252}Cf . Based on simulations, such a count rate requires an average $[\text{}^6\text{Li}] = 0.37\%$, which is likely quite close to the actual crystal value given that the crystal ends are 0.25 and 0.47%.

DISCUSSION AND CONCLUSIONS

Saint-Gobain Crystals is industrializing large dual neutron/gamma scintillation detectors. A 120 liter, proof-of-concept, large NaI(Tl) ingot co-doped with ^6Li has been grown. A proof-of-concept, large (2000 cm^3) crystal detector cut from this ingot shows excellent neutron/gamma discrimination and reasonable gamma detection performance. The gamma detection performance can be increased with improved [Li] uniformity or with an overall increase in [Li]. Both techniques will be attempted in future growths. The neutron detection efficiency scales with $[\text{}^6\text{Li}]$ as expected from simulations. The promise of detectors available in large volumes makes NaIL a unique and useful fit for a variety of security applications.

For example, a typical ^3He neutron detector used in vehicle scanning at U.S. borders (i.e. “portal” monitors) are of size $\varnothing 5 \times 173 \text{ cm}$ and pressurized to 3 atm. A typical neutron detection efficiency for these detectors is $\sim 3.0 \text{ count/s/ng } ^{252}\text{Cf}$ at 2 m¹⁵. Thus, three large NaIL detectors like that shown in Figure 6 with $[\text{}^6\text{Li}]$ increased to 1% should have almost the same efficiency as an ^3He tube (i.e. $0.40 \text{ cps/ng} \times 1\% / 0.37\% \times 3 = 3.2 \text{ cps/ng}$). The cost is expected to be similar to one ^3He tube, but the NaIL detectors would have the benefit of adding gamma ray spectroscopy and isotope identification.

REFERENCES

- ¹ Kouzes, R. T. "the He-3 Supply Problem," PNNL-18388, Pacific Northwest National Laboratory, 2009.
- ² van Loef, E. V. D., Dorenbos, P., van Eijk, C. W. E., Kramer, K. W. & Gudel, H. U. , "Scintillation and spectroscopy of the pure and Ce³⁺-doped elpasolites: Cs₂LiYX₆ (X = Cl, Br)," *J. Phys. Condens. Mater.*, vol. 14, 8481-8496, 2002.
- ³ Glodo, J., Brys, W., Entine, G., Higgins, W. H., van Loef, E. V. D., Squillante, M. R. & Shah, K. S., "Cs₂LiYCl₆:Ce Neutron Gamma Detection System," in *Proc. IEEE Nuclear Science Symp. Medical Imaging Conf.*, vol. 2, 959-962, 2007.
- ⁴ Glodo, J., R. Hawrami, R., van Loef, E. V. D., Shirwadkar, U. & Shah, K. S., "Pulse Shape Discrimination With Selected Elpasolite Crystals," *IEEE Trans. Nucl. Sci.*, vol. 59, no. 5, 2328-2333, 2012.
- ⁵ Yang, K., Menge, P.R., Lejay, J. & Ouspenski, V., "Scintillation properties and temperature responses of Cs₂LiLaBr₆:Ce³⁺," in *Proc. IEEE Nuclear Science Symp. Medical Imaging Conf.*, 1-6, 2013.
- ⁶ Yang, K. & Menge, P. R., "Pulse shape discrimination of Cs₂LiYCl₆:Ce³⁺ scintillator from -30oC to 180 oC," *Nucl. Instrum. Methods Phys. A*, vol. 784, 74-79, 2015.
- ⁷ "CLYC-Configurations-5-10-16." (2016, May 10). Retrieved May 16, 2017, from <http://rmdinc.com/wp-content/uploads/2016/06/CLYC-Configurations-5-10-16.pdf>
- ⁸ Yang, K. & Menge, P. R., "Li co-doped NaI:Tl+ - A Large Volume Neutron-Gamma Dual Mode Scintillator with Exceptional Pulse Shape Discrimination," *IEEE Nuclear Science Symp. Medical Imaging Conf.*, 2016.
- ⁹ Winyard, R.A., Lutkin, J. E. & McBeth, G. W., "Pulse shape discrimination in inorganic and organic scintillators. I," *Nucl. Instrum. Methods Phys. A*, vol. 95, no. 1, 141-153, 1971.
- ¹⁰ Yang, K., Menge, P.R., & Ouspenski, V., "Li co-doped NaI:Tl (NaIL) – A Large Volume Neutron-Gamma Scintillator with Exceptional Pulse Shape Discrimination," submitted to *IEEE Trans. Nucl. Sci.*, January 2017.
- ¹¹ Sangster, J. M. & Pelton, A. D., "Phase diagrams and thermodynamic properties of the 70 binary alkali halide systems having common ions," *J. Phys. Chem. Ref. Data*, vol. 16, no. 3, 509-561, 1987.
- ¹² Wolski, D., Moszynski, M., Ludziejewski, T., & Skeppstedt, O., "Comparison of n-γ discrimination by zero-crossing and digital charge comparison methods," *Nucl. Instrum. Methods Phys. A*, vol. 360(3), 584-592, 1995.
- ¹³ Pelowitz, D. B., Ed., "MCNPX Users Manual Version 2.7.0," LA-CP-11-00438, Los Alamos National Laboratory (2011).
- ¹⁴ Sears, F. V., "Special Feature - neutron scattering lengths and cross sections," *Neutron News*, vol. 3, no. 3, 29-37, 1992.
- ¹⁵ Kouzes, R. T., Ely, J. H., Lintereur, A. T., Siciliano, E. R., Stromswold, D. C., Woodring, M. L., "He-3 Neutron Detector Pressure Effect and Comparison to Models," PNNL-19110, Pacific Northwest national Laboratory, 2010.